Photofragment Imaging of CH_3Br^+ from $(CH_3Br)_2^+$ at 355 nm

Kunihiro Suto, Yoshihiro Sato, Yutaka Matsumi, and Masahiro Kawasaki*

Institute for Electronic Science, and Graduate School of Environmental Science, Hokkaido University, Sapporo 060, Japan

Received: September 24, 1996; In Final Form: November 25, 1996[⊗]

Photodissociation of $(CH_3Br)_2^+$ was studied at 355 nm with photofragment imaging spectroscopy for the product CH_3Br^+. The center-of-mass translational energy distribution is represented by a Gaussian distribution that peaks at 25 kcal mol^{-1}. The angular distribution is characterized by the anisotropy parameter $\beta = 1.8 \pm 0.2$. Photodissociation dynamics of the ion dimer at 355 nm is discussed.

Introduction

The photodissociation dynamics of dimer cations for NO_2, N_2, CO_2, and benzene in the visible region was reported by the groups of Bowers[1−3] and Nishi,[4] measuring translational energy and angular distributions of the fragments. For $(N_2)_2^+$, $(NO)_2^+$, and $(CO_2)_2^+$, the facts that (a) the kinetic energy increases linearly with the available energy and (b) the large anisotropy parameter β for spatial angular distribution can be accounted for by using a simple impulsive model for a direct dissociation path on a repulsive potential surface.[1−3] For $(C_6H_6)_2^+$, however, the translational energy distribution is statistical with $\beta = 0$, suggesting fast energy flow among the intramolecular vibrational modes.[4] They found that the slope of the averaged translational energy plotted against the available energy is in the order $(NO)_2^+$, $(N_2)_2^+ > (CO_2)_2^+ \gg (C_6H_6)_2^+$, in other words, the greater the number of internal degrees of freedom, the smaller the kinetic energy release. Since a further study on the photodissociation dynamics of the dimer of middle-size molecules is required, the photodissociation of $(CH_3Br)_2^+$ has been studied by ion-imaging spectroscopy, with which the kinetic and angular distributions of the photofragment can be measured simultaneously.

Experimental Section

The experimental apparatus is essentially the same as that reported by Chandler and Houston,[5] which consists of three differentially pumped chambers and was described elsewhere.[6] The molecular beam and reaction chambers are pumped by separate 6 in. diffusion pumps. The detection chamber is pumped with a turbo molecular pump. The three axes, molecular beam, laser beam, and detector, are orthogonal in the interaction region. The 118 nm light is generated by tripling of the 355 nm output (5−10 mJ/pulse) of a Nd^+:YAG laser (Quanta Ray) in a tripling cell with 10−20 Torr of Xe gas with a quartz lens ($f = 150$ mm at 355 nm). The tripling cell is schematically shown in Figure 1. The 118 nm light generated is focused with a LiF lens into the interaction region so that the pulsed molecular beam of CH_3Br (2.5−10%) in Ar or He at stagnation pressure of 700 Torr is photoirradiated by both 118 and 355 nm laser light with a pulse molecular beam head and driver (General Valve). Due to the large difference in the focal length of the LiF lens at 118 and 355 nm ($f = 50$ and 80 mm at 118 and 355 nm, respectively), the 355 nm light is focused further away from the interaction region. Thus, multiphoton processes by the 355 nm light are eliminated at the interaction region. Actually, without Xe gas in the cell, no signals were observed. The signal ions produced in the interaction region are accelerated into the time-of-flight (TOF) tube by a 2 kV electrode, fly through a field-free region of 500 mm, and strike a multichannel plate (MCP, Hamamatsu Photonics, 40 mm diameter) that is equipped with a fast phosphor screen at the end of the TOF tube. A CCD camera (Hamamatsu Photonics) attached with a gated image intensifier observes the image on the phosphor screen through a lens. The image signal from the camera is accumulated in a microcomputer over 12 800 laser pulses. In the photofragment imaging experiment, the three-dimensional (3-D) velocity distribution is projected onto a two-dimensional (2-D) detector. To extract a 3-D distribution from a 2-D image, we use a filtered back-projection technique,[7] which was described elsewhere.[6] Velocity resolution of an obtained image is determined by measurement of the images of photofragments from the photodissociation of I_2 and ICl at 304 nm. Time-of-flight spectra of the ions are measured by monitoring the ion current from the phosphor plate on the MCP.

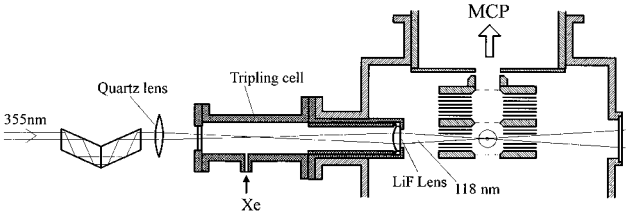

Figure 1. Schematic of the interaction region of the ion imaging apparatus. Detection and molecular beam chambers are not shown here and were reported previously.[6]

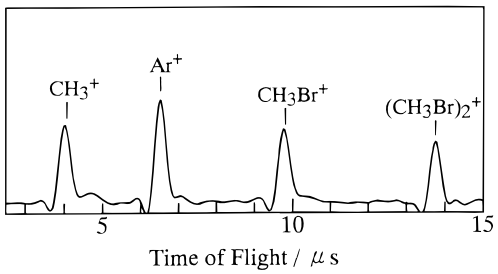

Figure 2. Time-of-flight mass spectrum following photoirradiation of pulsed molecular beam of CH_3Br (10%) in Ar (700 Torr) at 118 and 355 nm.

Results

Figure 2shows the ion TOF spectrum, in which CH_3^+, Ar^+, CH_3Br^+, and $(CH_3Br)_2^+$ appear: CH_3^+ were deduced to come

[⊗] Abstract published in *Advance ACS Abstracts,* January 15, 1997.

S1089-5639(96)02930-1 CCC: $14.00

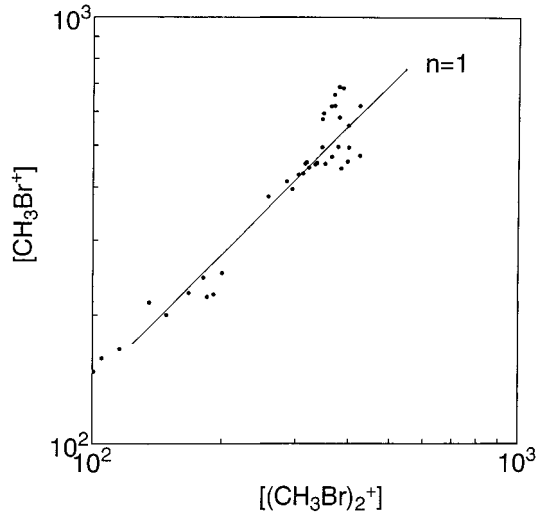

Figure 3. Ion intensity of CH_3Br^+ as a function of $(CH_3Br)_2^+$ intensity. The total stagnation pressure is 600−760 Torr, and the concentration of CH_3Br is varied from 2.5 to 10%. The slope of the line is unity. The *x* and *y* axes are in arbitrary units.

from the ion-pair dissociation process of CH_3Br as was reported earlier by Munakata and Kasuya,[8] Ar^+ from a multiphoton process, and CH_3Br^+ from photodissociation of $(CH_3Br)_2^+$ as will be discussed below. To confirm the $(CH_3Br)_2^+$ dimer dissociation pathway for CH_3Br^+ production, we tested various concentrations of CH_3Br (2.5−10%) in Ar for the molecular beam. Figure 3shows a log−log plot of the CH_3Br^+ signal intensity as a function of $(CH_3Br)_2^+$ signal intensity. The slope of this plot is almost unity, indicating that it is the $(CH_3Br)_2^+$ which are most important to CH_3Br^+ photoproduction. Since the ionization potential of CH_3Br is 10.56 eV, which is slightly higher than the photon energy of 10.483 eV at 118.27 nm, most of the CH_3Br^+ signals come from dissociation of the dimer ions but not directly from ionization of the monomers. Since CH_3^+ are known to come from the ion-pair dissociation of the monomers at 118 nm,[8] the intensity of CH_3^+ is a measure of the monomer concentration in the molecular beam. At various concentrations of CH_3Br in the gas reservoir for the molecular beam, a quadratic dependence of CH_3Br^+ intensity on the CH_3^+ signal intensity was observed, which is due to the participation of the dimers in the production of CH_3Br^+. Absence of the CH_3Br^+ signals from $CH_3Br{\cdot}Ar$ clusters was verified by the fact that when He gas was used as a buffer gas, there was no marked difference in the observed image of CH_3Br^+ from that observed with Ar. These results suggest little contribution of the complex between CH_3Br and the carrier gas to the formation of CH_3Br^+.

The 118 nm laser light was focused at the interaction region, whereas the 355 nm light was not focused there. When the 118 nm generation was removed by evacuating the Xe tripling cell, none of these signals were produced. Hence, CH_3Br^+ were produced by one-photon ionization of the dimer at 118 nm, followed by one-photon dissociation at 355 nm at the interaction region:

$$(CH_3Br)_2 + h\nu(118.27\ \text{nm}) \rightarrow (CH_3Br)_2^+ + e^- \quad (1)$$

$$(CH_3Br)_2^+ + h\nu(354.8\ \text{nm}) \rightarrow CH_3Br^+ + CH_3Br \quad (2)$$

The images of CH_3Br^+ are shown in Figure 4, in which the laser light beam was polarized in the plane as shown by an arrow. The upper panel of Figure 4 shows a 2-D image obtained experimentally, and the lower one shows a 3-D backprojected

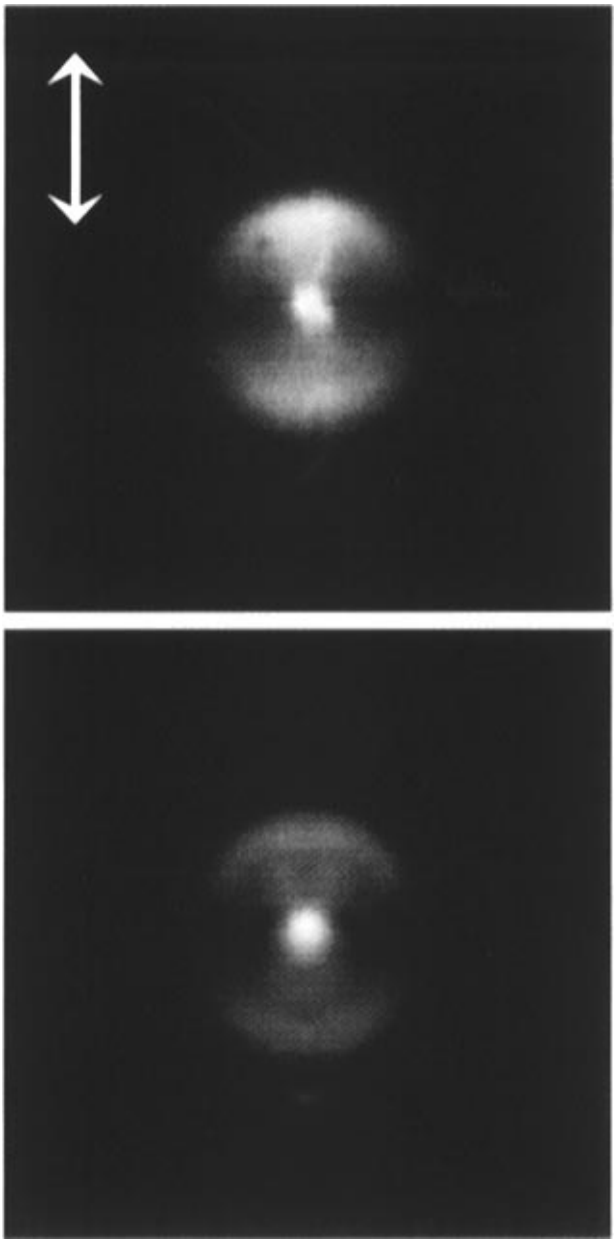

Figure 4. Images of CH_3Br^+ ions following photoirradiation of CH_3Br pulsed molecular beam simultaneously at 118 and 355 nm: (top) raw image; (bottom) back-projected image. An arrow indicates the direction of the electric vector of the dissociation laser at 355 nm.

image, which is an equatorial slice of the 3-D distribution. The speed distribution $v^2f(v)$ is obtained from the radial distribution of an image and then converted to the distribution of center-of-mass translational energy E_t as shown in Figure 5. The energy distribution is resolved into three parts: one is the highest energy component represented by a Gaussian distribution (peak = 25 kcal mol^{-1} and fwhm = 17 kcal mol^{-1}), the middle energy component represented by another Gaussian (peak = 8 kcal mol^{-1} and fwhm = 8 kcal mol^{-1}), and the rest is represented by a Boltzmann with temperature of 400 K. Since the instrumental velocity resolution corresponds to energy resolution of 6 kcal/mol at the peaks, fwhm are corrected for their widths.

The angular distribution at a certain speed is fitted by

$$I(v,\theta) = (1/4\pi)f(v)\{1 + \beta P_2(\cos\theta)\} \quad (3)$$

where θ is the angle between the polarization vector of the dissociation laser and the velocity vector of the fragment. β is an anisotropy parameter, and $P_2(x)$ is the second Legendre

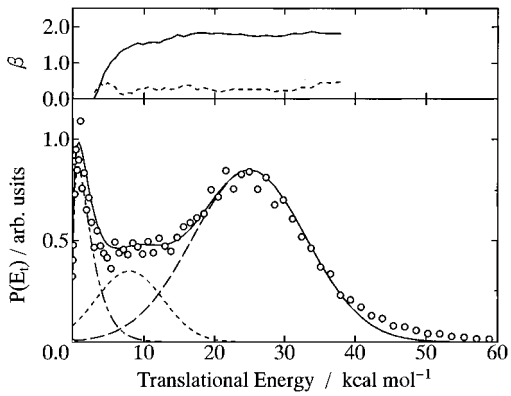

Figure 5. Center-of-mass frame translational energy distribution $P(E_t)$ (bottom) and anisotropy parameter $\beta(E_t)$ (top). The translational energy distribution is reproduced by three different distributions: two Gaussian peaking at 25 and 8 kcal mol^{-1} and a Boltzmannian characterized by a temperature of 400 K. A broken curve in the figure of $\beta(E_t)$ shows standard errors (1σ) for β.

polynomial defined as $P_2(x) = {}^1/_2(3x^2 - 1)$. For recoil along the breaking dimer bond, the two limiting cases are recoil parallel to μ or $\beta = 2$, and recoil perpendicular to μ or $\beta = -1$.[9] Our experimental results for β values are 1.8 ± 0.2 as shown in Figure 5 as a function of E_t. The β value is close to the upper limit of 2 at the higher energy region ($E_t > 15$ kcal mol^{-1}), while at the lower energy region (<10 kcal mol^{-1}) the β value approaches 0. This low β value is due to a mixing of the outer ring image with the center image. The center image of Figure 4 is caused mostly by the 118 nm photoionization of vibrationally hot parent CH_3Br molecules and not photofragment signals from the dimer ions, because the β value of the center image is 0 and its translational energy is well characterized by a Boltzmann temperature of 400 K. Since the outermost image or the highest energy component that is represented by the Gaussian distribution contributes the most to the dissociation process of the dimer ion, we will focus our discussion on the dynamics of this major process.

The analogous experiment at 118 nm was performed for CH_3I and CH_3Cl without success. A strong image signal of CH_3I^+ and a weak one of CH_3Cl^+ were observed, both of which have only a low translational energy component. Because the ionization potential (Ip = 9.54 eV) of the parent molecule CH_3I is lower than the photon energy, CH_3I^+ were produced by the one-photon ionization at 118 nm. The photofragment ion CH_3I^+ could not be separated from the strong one-photon ionization signal, even if the photofragment was produced by the ion-pair dissociation process. Since the Ip of CH_3Cl (11.28 eV) and hence that of the dimer are much higher than the 118 nm photon energy, the dissociation of the dimer ion was not observed for CH_3Cl. Only a multiphoton process gave a weak center image of CH_3Cl^+.

Discussion

A. Bond Dissociation Energy. The large β value for the outer image, that is, the high-energy component is very suggestive of a fast direct dissociation from a repulsive surface that is analogous to photodissociation of simple dimer ions,[1−3] $(NO)_2^+$, $(N_2)_2^+$, and $(CO)_2^+$. The reported β values are 1.3 for $(NO)_2^+$, 1.15−1.35 for $(N_2)_2^+$, and 1.0 for the high-energy component from $(CO_2)_2^+$. This feature is characteristic of the dissociation occurring in a repulsive potential surface. For these molecules, the energy partitioning can be accounted for by using a simple spectator stripping model.[2] In this model, the translational energy release is given by

$$E_t = (\mu_{BC}/\mu_F)(E_{avl} - E_{vib})$$
$$E_{avl} = h\nu - D_0 \quad (4)$$

where μ_{BC} is the reduced mass of the atoms at the end of the breaking bond, μ_F is the reduced mass of the fragments, D_0 is the bond dissociation energy, and E_{vib} is the vibrational energy of the fragments which arises from geometry changes on going from reactant to products. Since the maximum translational energy of Figure 5 is 2.2 eV, the maximum value of D_0 for $(CH_3Br)_2^+$ is 0.86 eV based on the energy conservation. According to Meot-Ner[10] the D_0 value for $CH_3NH_2\cdots BrCH_3$ is 0.49 eV. Since the Br atom has a large ion size and its electrostatic interaction is large, the D_0 value for the Br···Br bond in the dimer ion should be larger than 0.49 eV. The dimer binding energies are not expected to be vastly different among the various species. The D_0 values for $(CO_2)_2^+$, $(NO)_2^+$, $(C_2H_2)_2^+$, $(C_2H_4)_2^+$, and $(C_6H_6)_2^+$ are similar to each other in these molecules: 0.7,[3] 0.598 ± 0.06,[11] 0.98 ± 0.04,[12] 0.69 ± 0.04,[12] 0.663 ± 0.039 eV.[13] Thus, we estimate $D_0 = 0.7 \pm 0.2$ eV for $(CH_3Br)_2^+$. Using this value and the averaged translational energy $\langle E_t \rangle$ of 1.08 eV (25 kcal mol^{-1}) for the fast Gaussian component in Figure 5, the fraction of the available energy released into translation is estimated to be 0.39 ± 0.03, which is smaller than 0.47 for $(N_2)_2^+$ [1] and 0.51 for $(NO)_2^+$.[2] Assuming the impulsive model of eq 4 that holds for the fast dissociation process the value of E_{vib} is estimated to be 1.2 eV (28 kcal mol^{-1}), suggesting strong vibrational excitation of the fragment(s).

B. Ionization and Dissociation Processes. The ionization process removes an electron from a nonbonding π orbital on a Br atom. The resulting electron hole is delocalized between the two Br atoms which explains the lowering of the ionization potential (Ip) of the dimer as compared to that of the monomer. The Ip of CH_3Br is 10.53 eV, and the energy of the 118.2 nm ionizing photon is 10.49 eV. The magnitude of the lowering of the Ip depends on the unknown distance between Br atoms in the neutral dimer. While the dimer structure is unknown, it is helpful to compare this system with a simpler one. The Ip's of the Br atom and the Br_2 molecule are 11.84 and 10.54 eV, respectively. This lowering of 1.30 eV is probably an upper limit to the lowering of the Ip of the CH_3Br dimer. Whatever the initial structure of the neutral dimer is, both Br atoms in the charged dimer would come into close contact with each other so as to maximize the stabilization energy of the resonant charge transfer.

Once formed, the ionized dimer is dissociated by polarized 355 nm light. The velocity distribution of the fragment peaks in a direction parallel to the electric vector of the polarized light. The equal and opposite velocities of the CH_3Br and CH_3Br^+ fragments make only a small angle with respect to the Br···Br axis because the Br atoms are more than 5 times heavier than the CH_3 groups. We can therefore state that the transition dipole direction is parallel to the Br···Br axis. This is what we would expect for a (π,π^*) transition, in which a bonding π electron is excited into the π^* hole.

The average translational energy release observed in the photodissociation is around 1.1 eV. The rotational energy is expected to be negligible because the center of mass of the CH_3-Br is so close to the Br atom that the repulsive force exerted between the Br atoms cannot generate much rotational energy. Assuming a impulsive rigid-rotor model for separation of the two fragments, the maximum fraction of available energy released into rotation is 17%. The bond dissociation energy of the Br···Br bond in the dimer is estimated to be 0.7 eV according to the arrangement given previously. Thus, the average

vibrational energy is greater than 1.7 eV, based on the conservation of energy for the dissociation process. Impulsive model of eq 4 predicts $E_{vib} = 1.2$ eV. This large vibrational energy may result from the fact that the two equivalent C−Br bonds of the charged dimer become two inequivalent bonds, one shorter and one longer.

Using He I photoelectron−photoion coincidence measurement, Lane and Powis[14] reported that the direct ionization of the neutral ground states of CH_3Br at 13.8−14.5 eV prepares highly vibrationally excited A state of the monomer CH_3Br^+ ions. The A-band ionization of this molecule is a removal of a C−Br bonding electron.

Acknowledgment. M.K. and Y.M. acknowledge Grants-in-Aid from the Ministry of Education, Science, Culture and Sports of Japan, in the priority field of "Photodynamics" and in the field of General Chemisty, respectively. The authors thank Prof. Richard Bersohn of Columbia University for discussion on the dissociation process and Mr. Y. Hirata and T. Meike for their help in construction of the imaging machine.

References and Notes

(1) Jarrold, M. F.; Illies, A. J.; Bowers, M. T. *J. Chem. Phys.* **1988**, *79*, 6086.

(2) Jarrold, M. F.; Illies, A. J.; Bowers, M. T. *J. Chem. Phys.* **1984**, *81*, 214.

(3) Illies, A. J.; Jarrold, M. F.; Wagner-Redeker, W.; Bowers, M. T. *J. Phys. Chem.* **1984**, *88*, 5204.

(4) Ohashi, K.; Nishi, N. *J. Chem. Phys.* **1993**, *98*, 390.

(5) Chandler, D. W.; Houston, P. L. *J. Chem. Phys.* **1987**, *87*, 1445.

(6) Sato, Y.; Matsumi, Y.; Kawasaki, M.; Tsukiyama, K.; Bersohn, R. *J. Phys. Chem.* **1995**, *99*, 16307.

(7) Budinger, T. F.; Gullberg, G. T. *IEEE. Trans. Nucl. Sci. NS* **1974**, *21*, 2.

(8) Munakata, T.; Kasuya, T. *Chem. Phys. Lett.* **1992**, *154*, 604.

(9) Zare, R. N.; Herschback, D. R. *Proc. IEEE.* **1963**, *51*, 173.

(10) Meot-Ner, M. *J. Am. Chem. Soc.* **1984**, *106*, 1257.

(11) Lin, S. H.; Ono, Y.; Ng, L. Y. *J. Chem. Phys.* **1981**, *74*, 3342.

(12) (a) Ono, Y.; Ng, C.-Y. *J. Chem. Phys.* **1982**, *77*, 2947. (b) Ono, Y.; Linn, S. H.; Tzeng, W.-B.; Ng, C. Y. *J. Chem. Phys.* **1984**, *80*, 1482.

(13) Snodgrass, J. J.; Dunbar, R. C.; Bowers, M. T. *J. Phys. Chem.* **1990**, *94*, 3648.

(14) Lane, I. C.; Powis, I. J. *J. Phys. Chem.* **1993**, *97*, 5803.